Electric Power Systems Research 190 (2021) 106611

Contents lists available at ScienceDirect

Electric Power Systems Research

journal homepage: www.elsevier.com/locate/epsr

Computation of sensitivity-based islanding detection parameters for synchronous generators

Tin Rabuzin*, Fabian Hohn, Lars Nordström

Division of Electric Power and Energy Systems, KTH Royal Institute of Technology, Stockholm, Sweden

ARTICLE INFO

Keywords:
Distributed generation
Islanding detection
Kalman filter
Least squares
Sensitivity computation

ABSTRACT

Significant penetration levels of distributed energy resources increase the likelihood of continued operation of a power system island after an islanding event. It is important to employ adequate islanding detection methods to mitigate the adverse effects of unintentional islanding and possibly transition to a safe islanded mode of operation. This paper focuses on the computational aspects of a class of methods that utilizes a change in the sensitivity parameters as an indicator of islanding events. It is shown that the inherent properties of the measurement signals cause numerical issues for the computation of the sensitivity parameters. The paper also analyses three algorithms for estimation of the coefficients that overcome the numerical issues. The performance of the algorithms has been demonstrated using synthetically generated measurements. In addition, the data from field experiments has been used to further illustrate the practical viability of the algorithms.

1. Introduction

The reduction of greenhouse gas emissions through sustainable and efficient energy production has been one of the targets of the European 2020 strategy [1]. Many of the EU countries have adopted and implemented measures to achieve the 2020 targets. For example, Sweden reports that 54% of its generated electric power in 2017 originated from renewable energy sources [2]. The aforementioned environmental goals, along with the technological developments and economic opportunities, have facilitated the integration of distributed energy resources (DERs) in distribution networks [3]. Despite many benefits that DERs bring, several adverse effects on the utility grids caused by DERs have been observed, one of which is the possibility of islanding [4].

Power system islanding is an event that causes a part of a network to be electrically separated from the utility grid and, subsequently, the newly created electrical island continues to be energized by local DERs. Unintentional islanding events can have a negative influence on the safe and stable operation of a network. If unintentional islanding is not detected, it can endanger line workers, cause unsynchronised reclosing or impair the voltage and frequency control in the island [5]. To prevent the consequences of islanding and possibly ensure a safe transition to an islanded mode of operation, a quick and reliable islanding detection method (IDM) is needed.

IDMs can be broadly classified into local and remote techniques [6]. Local IDMs can be further classified into passive and active methods. Passive IDMs base their algorithms on a detectable change in the measurements of the system's electrical quantities after islanding, such as rate of change of frequency (ROCOF), rate of change of active power [7], rate of change of output power over frequency [8], vector shift, and under/over voltage [9]. The inherent drawback of passive methods is the existence of a non-detection zone (NDZ), i.e. the passive methods fail to detect islanding if the imbalance of the production and consumption in an island is sufficiently small [10].

Active methods have been utilized to reduce the NDZ by introducing non-destructive perturbations to the system. It is assumed that the perturbations disturb the balance in the island and cause a detectable change in the system's response, when a DER is islanded. While active methods have a smaller NDZ compared to passive methods, they might cause undesirable system disturbances. Furthermore, interference issues may arise if more than one DER employs an active detection method in an island[11]. The active methods which are applicable to the case of synchronous generators are reactive export error detection [12], impedance monitoring [13], and the methods introducing positive feedback loop to the generator's control systems [14].

Remote techniques rely on the ability of acquiring distant measurements or signals. Examples of such IDMs are comparison of ROCOF [15], transfer-trip schemes [16], power line signaling [17], and slip frequency and angle method [18]. These methods typically have smaller NDZs when compared to local methods, but the cost of communication infrastructure often makes remote methods economically

* Corresponding author.
E-mail addresses: rabuzin@kth.se (T. Rabuzin), fhohn@kth.se (F. Hohn), larsno@kth.se (L. Nordström).

https://doi.org/10.1016/j.epsr.2020.106611
Received 27 September 2019; Received in revised form 14 February 2020; Accepted 31 July 2020
Available online 04 August 2020
0378-7796/

infeasible.

This paper focuses on a class of local IDMs, such as those discussed in [8,12], and [19] that use computed sensitivity coefficients of the generator's electrical quantities. Although the use of these IDMs had been shown to be promising, the practical implementation aspects of the computational algorithms have been overlooked. However, sensitivity coefficients have previously been used, mainly for voltage stability and control problems, and different methods have been developed to compute them from measurements. For example, in Leelaruji et al. [20] the sensitivities have been computed by low pass filtering and differentiation of the measurements smoothed by a moving average filter. Furthermore, Chen et al. [21] proposes a least squares approach to computing sensitivity parameters. A generalized least squares method has been used in [22] and [23] proposes to use compressed sensing to estimate sensitivities.

One of the contributions of this paper is to identify the challenges in computing the sensitivity coefficients and demonstrate how these challenges can degrade the performance of the discussed class of IDMs. When compared to previously proposed sensitivity estimation approaches, the intended application of the computed coefficients and the associated requirements are different in this paper. Therefore, the paper analyses three estimation algorithms which can successfully estimate the coefficients considering the following conditions.

Firstly, we assume that only local measurements are available and that they are reported at higher rates than the measurements from phasor measurement units (PMUs) or smart meters as in [21–23]. Furthermore, this paper assumes the existence of a weak although persistent system excitation originating from perturbations of generators' reference values. The estimation algorithms also need to be capable of real-time execution, to provide fast tracking of sensitivity coefficients to avoid out-of-step reclosing and to operate successfully under the assumptions stated above.

In addition, the paper evaluates the performance of the algorithms both by synthetically generated measurements and real measurements taken at a synchronous generator in a distribution network during islanding experiments.

2. Problem definition

Consider an equivalent model of a synchronous generator connected to a network at the point of common coupling (PCC) as depicted in Fig. 1. There are two main control systems at every synchronous generator; the one involving an automatic voltage regulator (AVR) and an exciter, and the other comprised of a turbine and a governor. Using these two systems, small perturbations to the references of the active power, reactive power or voltage can be introduced.

We consider a case in which one of the references is continuously perturbed using a small nondestructive periodic signal in order to ensure persistent excitation of the system. The response of the system is measured at the terminals of the generator based on which the sensitivity parameters, introduced in the following subsection, can be computed. The change in the response of the system, reflected in the change of the sensitivity parameters, can serve as an indication of an islanding event.

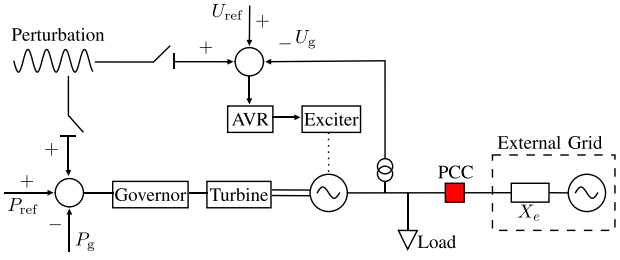

Fig. 1. Unintentional islanding test configuration.

2.1. Sensitivity parameters

The sensitivity parameters, which can be computed from the system's response, are:

- rate of change of frequency over active power
- rate of change of active power over voltage
- rate of change of reactive power over voltage
- rate of change of reactive power over frequency

While all of the parameters above produce a change in their value upon islanding, this paper further analyses the rate of change of reactive power over voltage as a representative case due to its physical interpretability. Moreover, the reactive power and voltage control loops produce faster responses to the changes of the reference values due to the smaller time constants involved in the control loops resulting in faster islanding detection.

The reactive power produced by a generator connected to a network approximated by its Thévenin equivalent is:

$$Q_g = \frac{U_g^2 - U_g E\cos(\varphi)}{X_e}, \tag{1}$$

where E and X_e are the Thévenin-equivalent voltage magnitude and reactance, respectively. U_g is the generator's terminal voltage magnitude and φ is the angle difference between the generator terminal and the Thévenin-equivalent voltage. The sensitivity of the produced reactive power to changes in the generator's terminal voltage is:

$$\theta_q = \left.\frac{\partial Q_g}{\partial U_g}\right|_{\substack{U_g=U_{go}\\ Q_g=Q_{go}}} = \frac{2U_{go}}{X_e} - \frac{E\cos(\varphi)}{X_e} \tag{2a}$$

$$= \frac{U_{go}^2}{U_{go}X_e} + \frac{U_{go}^2 - U_{go}E\cos(\varphi)}{U_{go}X_e} \tag{2b}$$

$$= \frac{U_{go}}{X_e} + \frac{Q_{go}}{U_{go}}, \tag{2c}$$

with U_{go} and Q_{go} being the steady-state generator voltage and reactive power, respectively. Synchronous generators are typically operated close to unity power factor and thus the second element in (2c) is considered to be negligible. Furthermore, X_e in the grid-connected mode of operation is much smaller when compared to the islanded mode of operation. Therefore, the increase of the equivalent network reactance as seen from a generator after islanding causes a reduction in the sensitivity parameter, which indicates that an islanding event has occurred. Furthermore, by knowing the equivalent reactance of the network, a threshold for the sensitivity parameter can be determined

2.2. Computational issues

The detection parameters, listed in the previous subsection, can be generically represented as the following parameter:

$$\theta = \frac{\partial y(t)}{\partial x(t)}, \tag{3}$$

where the signals $x(t)$ and $y(t)$ can be any of the aforementioned measurements of the generator's electrical quantities.

The straightforward way of estimating the parameter θ in practical implementations is to perform approximations of the sensitivity parameter by finite differences of the sampled signals, $x(n)$ and $y(n)$, as follows:

$$\theta \approx \frac{y(n) - y(n-1)}{x(n) - y(n-1)} = \frac{\Delta y(n)}{\Delta x(n)}, \tag{4}$$

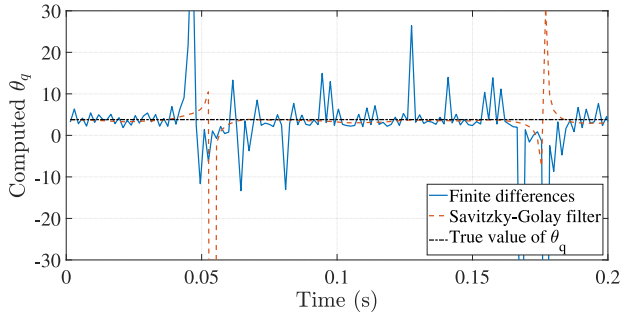

Fig. 2. Parameter θ_q computed by finite differences and SG filter .

such that $t = nT_s$ where T_s is sampling interval and $n \in \mathbb{Z}$. Performing numerical differentiation using (4) accentuates the omnipresent measurement noise, which can make the estimation of the parameter θ unreliable. Furthermore, the denominator of (4) may result in small quantities and if the algorithm is implemented using finite-precision arithmetic, this may result in memory overflows.

A snapshot of measurements was taken at a generator whose voltage reference was periodically perturbed, with the true value of the sensitivity parameter being $\theta_q \approx 3.8$. Fig. 2 shows the parameter θ_q estimated by (4) and by dividing measurements differentiated by the Savitzkey-Golay (SG) filter [24]. SG filtering is one of the possible ways of obtaining smoothed derivatives of a signal.

It can be observed that the finite difference method results in an unstable estimation of θ_q due to the presence of noise. SG filter somewhat improves the estimation of θ_q. However, similarly as in the case of finite differences, the division with the small values of the denominator, Δx, at some time instances causes spikes in the estimated parameter. This indicates that neither differentiation using finite difference nor differentiation using signal smoothing provide satisfactory results for an islanding detection application.

3. Estimation algorithms

The preceding section shows that there is a need for more suitable algorithms for the estimation of sensitivity parameters. Before presenting and discussing the estimation algorithms, the estimation problem is reformulated by manipulating (4) resulting in:

$$\Delta y(n) = \theta \Delta x(n) + v(n), \tag{5}$$

where it is assumed that the measurement errors of both $\Delta x(n)$ and $\Delta y(n)$ can be grouped and represented by white noise $v(n) \sim \mathcal{N}(0, \sigma_v^2)$. The implications of this assumptions are discussed in the following section. Using (5), sensitivity computation is restated as a minimization problem and as a state estimation problem in the following subsections.

3.1. Recursive least squares (RLS)

The least squares estimate of the parameter θ can be obtained by minimizing the following cost function:

$$f(\theta) = \sum_{i=1}^{N} [\Delta y(i) - \theta \Delta x(i)]^2, \tag{6}$$

where N is the number of available measurements. Differentiation of the cost function with respect to the parameter θ and setting the derivative equal to zero yields the least squares estimator:

$$\hat{\theta} = \left[\sum_{i=1}^{N} \Delta x(i)^2 \right]^{-1} \sum_{i=1}^{N} \Delta x(i) \Delta y(i). \tag{7}$$

The measurements in this application are acquired sequentially, which implies that the number of available measurements, N, grows with time thus requiring, in theory, an infeasible amount of memory. Furthermore, the parameter θ can change over time, conversely to the inherent assumption of the least squares estimator in (7).

To adapt the estimation for real-time execution and take into account the time-varying behavior of θ, the recursive least squares algorithm can be used. The RLS estimator is given by the following set of recursive equations [25]:

$$\begin{aligned} \hat{\theta}(n) &= \hat{\theta}(n-1) + R(n)^{-1} \Delta x(n) \\ &\quad \times [\Delta y(n) - \Delta x(n) \hat{\theta}(n-1)] \quad \text{(8a)} \\ R(n) &= \lambda R(n-1) + \Delta x(n)^2 \quad \text{(8b)} \end{aligned}$$

The forgetting factor λ is used to improve the tracking capability of the least-squares estimator. If $\lambda < 1$ more weight is given to newer measurements, i.e. older measurements are "forgotten".

3.2. Blockwise least squares (BLS)

As pointed out by the authors in [26], RLS suffers from slow tracking capabilities for time-varying system parameters. To overcome this drawback, one can compute the least squares estimates over a sliding window of measurements similarly as in (7) using:

$$\hat{\theta}(n) = \left[\sum_{i=n-WS+1}^{n} \Delta x(i)^2 \right]^{-1} \sum_{i=n-WS+1}^{n} \Delta x(i) \Delta y(i) \tag{9}$$

where WS is the window size. Using BLS, improved tracking speed is expected since all of the old measurements outside of the sliding window are not taken into account.

Typically, BLS would be computationally expensive in real-time applications due to the operation of matrix inversions involved in the estimation of vectors of parameters. In this application, all of the involved variables are scalars, and therefore the computational demand is much lower. However, compared to RLS, this approach does require more memory since WS measurements need to be stored at each time instant.

3.3. Kalman filter (KF)

The sensitivity parameter can also be computed by estimating the state of a discrete-time state-space model where parameter changes are modelled as a random walk:

$$\theta(n+1) = \theta(n) + w(n), \tag{10}$$

with white noise $w(n) \sim \mathcal{N}(0, \sigma_w^2)$, i.e. we consider (10) to be the state equation and (5) to be the output equation of the state-space model. The parameter θ, now treated as a state variable, can be estimated using the recursive KF equations:

$$\hat{\theta}(n) = \hat{\theta}(n-1) + K(n)[\Delta y(n) - \Delta x(n) \hat{\theta}(n-1)] \tag{11a}$$

$$K(n) = \frac{P(n-1)\Delta x(n)}{\sigma_v^2 + \Delta x(n)^2 P(n-1)} \tag{11b}$$

$$P(n) = P(n-1) - K(n)P(n-1)\Delta x(n) + \sigma_w^2 \tag{11c}$$

RLS can be viewed as an instance of a KF with specific assumptions about the noise variances, i.e. KF is a more general filter. Although the possibility of tuning noise covariances makes KF more flexible, this comes at the cost of higher computational complexity compared to RLS.

3.4. Blocking scheme

The linearisation of the system in (2) is valid only in the proximity of the equilibrium. Consequently, when the system experiences transitions, neither the model of the system in (5) nor the estimated values of θ will be valid. Therefore, a blocking scheme is needed to prevent maloperation of the IDM. To block the IDM during transients, we propose to use the RMS value of the residuals:

$$B(n) = \sqrt{\frac{1}{WS_b}\sum_{i=n-WS_b+1}^{n}\varepsilon(i)^2} \tag{12}$$

where $\varepsilon(n) = \Delta y(n) - \Delta x(n)\hat{\theta}(n-1)$ are the residuals obtained from the respective algorithms and WS_b is the window size over which $B(n)$ is calculated. If WS_b is set to be equal to the period of the injected perturbations and the threshold for $B(n)$ is set above its steady-state value, it is essentially required that the filters need to be in steady state over a period of the perturbation signal in order for the estimates to be considered valid.

4. Simulation and experimental results

This section presents test results used to evaluate the performance of the algorithms described in Section 3. We analyse convergence rates of the algorithms and the influence of measurement noise on the estimation results. Furthermore, the algorithms were tested using real measurements acquired during islanding events and the blocking scheme was tested using the measurements acquired during a synchronisation procedure of an asynchronous machine.

4.1. Convergence analysis

To compare the convergence properties of the estimation algorithms, the following synthetic measurements were generated:

$$Q(n) = Q_{go} + Q_m \sin(2\pi fTn) + e_q(n) \quad (13a)$$
$$U(n) = U_{go} + U_m \sin(2\pi fTn) + e_u(n) \quad (13b)$$

where $T = 1.5$ms is the sampling time interval and f is the frequency of the simulated sinusoidal perturbations with the period of 130ms. The vector of parameters $X = [Q_0 \;\; Q_m \;\; U_0 \;\; U_m]^T$ changes as follows:

$$X = \begin{cases} [0.05 \;\; 0.02 \;\; 1 \;\; 0.005]^T & \text{for } 0\,\text{s} \leq t < 1\text{s} \\ [0.01 \;\; 0.005 \;\; 1 \;\; 0.01]^T & \text{for } 1\,\text{s} \leq t < 2.5\text{s} \end{cases}$$

The change in the parameters effectively causes the true value of the sensitivity parameter to decrease from $\theta_q = 4$ to $\theta_q = 0.5$ at $t = 1$s. Zero mean white Gaussian noise processes (e_q and e_u) were added to both of the signals such that the signal-to-noise ratio (SNR) of the sinusoidal component of the signal for $t < 1$s is 37dB and 49dB for reactive power and voltage signals, respectively. Generated measurements were then differentiated and the algorithms were used to estimate θ_q. The parameters of the algorithms were tuned so that the mean and variance of the steady-state estimates for all of the algorithms were equal. This experiment was repeated 500 times and the arithmetic mean of the estimates of $\hat{\theta}_q$ was calculated at each time instant.

The results of this procedure are shown in Fig. 3.

It can be observed that BLS has the highest convergence rate due to the fact that the transient caused by a sudden change of θ_q is forgotten as soon as the sliding window moves past it. This is not true for the recursive algorithms, RLS and KF, since the transient is not "forgotten" as quickly as in the case of BLS. However, the error during the transition period of BLS is higher than in the case of RLS and KF. Furthermore, flexibility of KF when compared to RLS can be observed. Although both of the algorithms have the same average steady-state performance, the state covariance was tuned so that KF converges faster to the steady-state value than RLS.

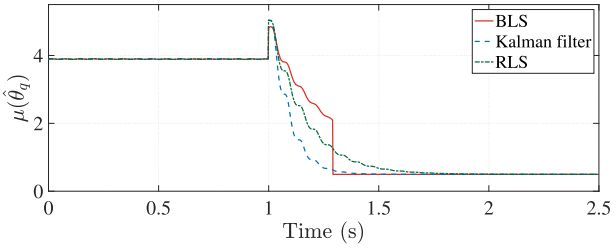

Fig. 3. Arithmetic mean of the estimated $\hat{\theta}_q$ over 500 experiments .

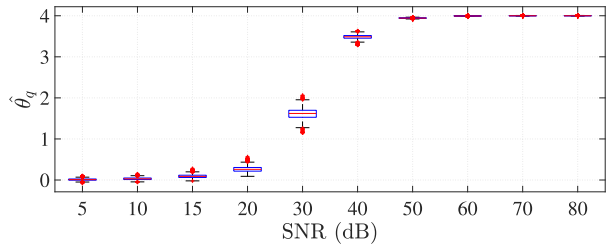

Fig. 4. Effect of noise in the independent variable on estimates of θ_q .

4.2. Influence of measurement noise

It can be observed in Fig. 3 that the estimates of all of the algorithms are biased, i.e. on average they do not result in the parameter's true value. The cause of the bias is the presence of noise in the measurements of the independent variable $\Delta x(n)$, which is not taken into account. This issue is known as errors-in-variables problem. However, the reliability of IDMs considered in this paper is not reduced if the bias present in the measurements is not significant, as shown below.

To quantify the impact of noise on the estimates, the system in 13 was simulated in steady-state, i.e. with no parameter changes with various SNRs. Fig. 4 shows a box plot of estimated values of θ with respect to different SNRs of the independent variable while keeping the SNR of the dependant variable, $\Delta y(n)$, fixed.

It can be observed that the increase of SNR of the independent variable reduces the bias in the estimates. In particular, SNRs higher than 40dB would not significantly reduce the reliability of the steady-state estimates. Similarly, Fig. 5 demonstrates the effect of SNR of the dependent variable on the estimates of θ while keeping SNR of the independent variable fixed.

The change of SNR of the dependant variable does not affect the bias of the estimates. However, the increase of SNR reduces the variance of the estimates, which increases their reliability.

4.3. Field measurements

The performance of the estimation algorithms was also tested by using measurements taken at a distribution level generator. The nominal power and voltage of the generator are $S_n = 20.5$MVA and $U_n = 11$kV, respectively. The true value of the sensitivity parameter as seen from the synchronous generator is $\theta_q \approx 3.8$. The thresholds for the estimated parameter $\hat{\theta}_q(n)$ and the blocking signal $B(n)$ were set to 1 and 0.001, respectively. To ensure persistent excitation, the generator voltage reference was being perturbed by a periodic signal of 4Hz.

The measurements of the reactive power and voltage used in the estimation of θ_q were obtained from the excitation system of the generator, which performs the following preprocessing steps. The AC stator voltage and current measurements are low-passed using a second order

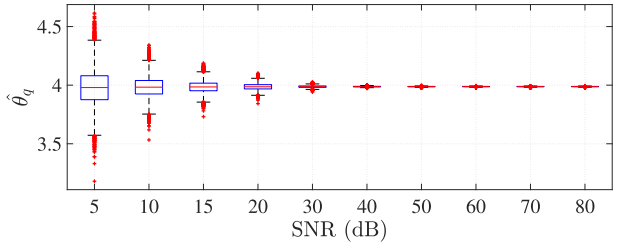

Fig. 5. Effect of noise in the dependent variable on estimates of θ_q .

Table 1
Islanding detection times for field data.

ΔP [kW]	t_{RLS} [ms]	t_{BLS} [ms]	t_{KF} [ms]
3	240	228	228
8	336	228	252
15	264	228	228
60	240	228	228
270	312	192	228

infinite impulse response (IIR) filter with a cutoff frequency at 600Hz. In the succeeding step, the RMS signals of the low-passed measurements are calculated and the produced reactive power is estimated. Lastly, second order band-stop IIR filters are applied to the RMS signals of the voltage and reactive power measurements with attenuated frequencies at 50Hz and 100Hz. In addition, the reactive power measurement is low-passed with a cutoff frequency at 100Hz. These band-rejected RMS voltage and reactive power measurements are the field measurements $U_g(n)$ and $Q_g(n)$, respectively, and considered in the following analysis. Note, that the perturbation frequency of 4Hz has been chosen in order to avoid impairments by the IIR filters.

A part of the distribution network to which the generator is connected was islanded with different values of power imbalance in the newly created island, listed in the first column of Table 1. Measurements of U_g and Q_g shown in Fig. 6 were taken during the islanding event with an active power imbalance in the island of $\Delta P \approx 3$kW.

These measurements were provided to the estimation algorithms presented in Section 3 and the estimation results are shown in Fig. 7.

It can be seen that the estimated values start decreasing after the islanding event. At the same time, the blocking signal $B(n)$ starts rising and blocks the operation of the islanding detection methods. After the initial transient, both the estimates of θ_q and $B(n)$ fall below the threshold levels, which results in a successful islanding detection.

The same tests were done for different imbalances in the created island and the detection times of the algorithms are shown in Table 1.

The detection times of BLS and KF are mostly influenced by the window size of the blocking scheme, WS_b, and thus the times do not differ much over different cases. This is, however, not the case for RLS, whose detection time is mostly influenced by its slower convergence rate.

To demonstrate the stability of the IDM, θ_q is estimated using field measurements taken during a synchronisation procedure of an asynchronous generator located at the same busbar as the synchronous machine. The measurements are shown in Fig. 8 and the estimation results in Fig. 9.

The results show stable estimates of θ_q until $t \approx 3.2$s when the synchronisation is started. During the synchronisation, estimates are considered to be invalid since $B(n)$ surpasses the threshold levels. When the steady-state is reached again, the estimates are above the threshold level resulting in the stable operation of the IDM.

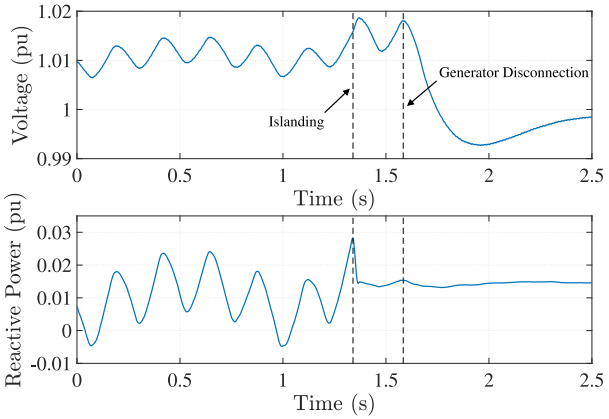

Fig. 6. Measurements during an islanding event with $\Delta P \approx 3$kW .

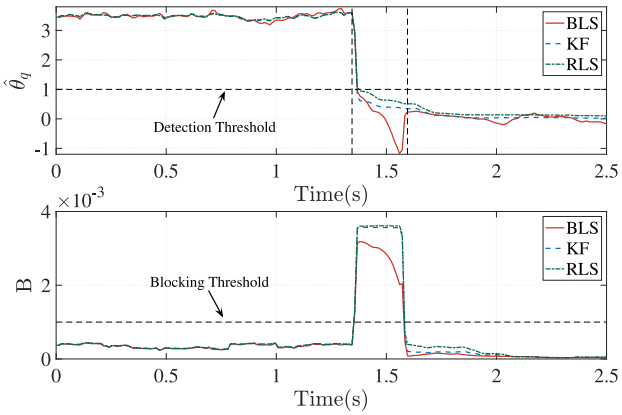

Fig. 7. Estimation of θ_q for an islanding event with $\Delta P \approx 3$kW.

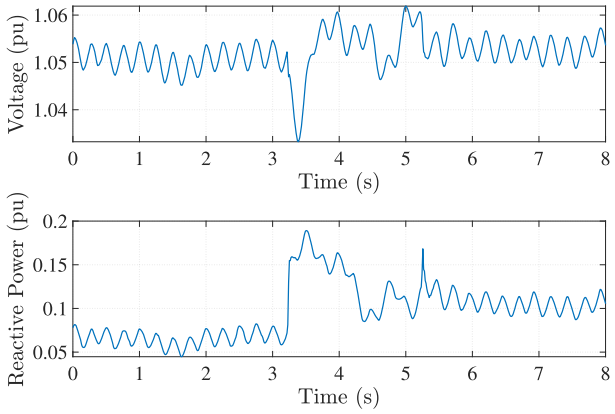

Fig. 8. Measurements during synchronisation of an asynchronous generator.

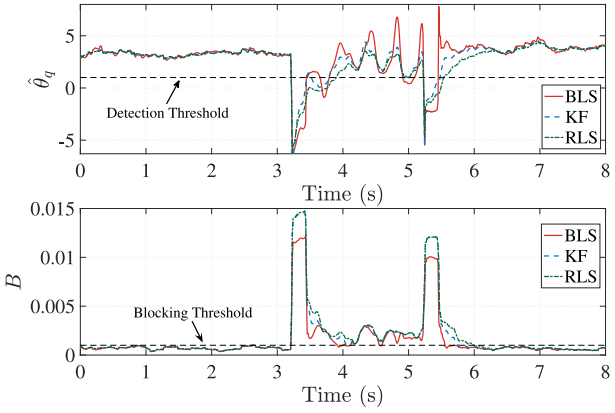

Fig. 9. Estimation of θ_q during synchronisation of an asynchronous generator.

5. Discussion

The preceding section demonstrates the performance of the estimation algorithms. First, it was shown that the tracking capabilities of different algorithms are not the same. Tuned such that the steady-state estimates are similar for all of the algorithms, the RLS was shown to be the slowest while KF and BLS perform similarly. However, the tracking capability is not the only measure by which the algorithms should be judged since the algorithms have to be augmented by a blocking

scheme in order to ensure stability during transients. It was shown that the islanding detection times, do not differ significantly between KF and BLS since they are mostly influenced by the window size used in the blocking scheme. However, the detection times of RLS were longer than both KF and BLS and influenced mostly by its poor tracking capability.

Furthermore, although it is possible to address the errors-in-variables problem with more complex algorithms such as total least squares, this is not necessary at sufficiently high SNR of the independent variable. It was shown that the bias is negligible above a certain level of SNR, which was also confirmed by accurate estimates of θ_q obtained from real measurements in steady-state.

The computational complexity and memory requirements of the algorithms have to be taken into account in real-time systems. RLS with the poorest tracking capability has the lowest computational and memory requirements. KF has higher computational and memory requirements than RLS but lower than BLS. Similarly to other protection functions, the design of an IDM has to balance between the dependency and stability of the method. The balance is reflected in the choice of the method and its hardware requirements as well as in the tuning of the algorithms' parameters.

One of the parameters that can significantly influence the performance of the method is the threshold for the sensitivity parameter. As shown in Section 2, it should be set according to the expected equivalent impedance of an islanded system which can vary with the current operation conditions of the network. Therefore, the threshold essentially determines the "size" of the island for which the IDM can operate.

6. Conclusions

This paper demonstrated the numerical challenges in computing the sensitivity parameters for islanding detection using local measurements. It also analysed the performance of three algorithms for sensitivity estimation that circumvent the numerical issues. The problem was formulated as an overdetermined system of linear equations for which the solution was obtained using the two least squares algorithms, and as a state estimation problem for which Kalman filter was used. Synthetic and field measurements were used to validate the algorithms. The results show that the longest detection times are obtained with RLS algorithm while BLS and KF perform similarly since they are constrained by the blocking function.

The problem formulation in this paper can serve as a basis for more complex IDMs where measurements from remote locations can be used. Furthermore, the interference issues in the system with multiple DGs that inject perturbations into the network can be analysed. Although the paper demonstrated the case of a synchronous generator, the same algorithms could be applied in the cases of inverter-interfaced production units. However, further work is need to evaluate the performance of the algorithms in these settings. Additionally, future work also includes refinements of the estimation algorithms by taking into account the discussed errors-in-variables problem and improvements of the blocking scheme by, e.g. performing whiteness tests.

Declaration of Competing Interest

The authors declare that they have no known competing financial interests or personal relationships that could have appeared to influence the work reported in this paper.

Acknowledgements

This work was supported by the SamspEL program of the Swedish Energy Agency. The authors would also like to thank Advensys Engineering Ltd. who provided the field measurements used in this work.

References

[1] European Commission (EC), Europe 2020: a strategy for smart, sustainable and inclusive growth, 2010. COM (2010) 2020.
[2] Swedish Energy Agency, Energy in Sweden - An Overview, 2019.
[3] G. Pepermans, J. Driesen, D. Haeseldonckx, R. Belmans, W. Dhaeseleer, Distributed generation: definition, benefits and issues, Energy Policy 33 (6) (2005) 787–798, https://doi.org/10.1016/j.enpol.2003.10.004.
[4] N. Jenkins, J. Ekanayake, G. Strbac, Distributed Generation, Energy Engineering Series, Institution of Engineering and Technology, pp. 12–18. 10.1049/pbrn001e.
[5] M. Bollen, F. Hassan, Integration of Distributed Generation in the Power System, IEEE Press Series on Power Engineering, Wiley, pp. 340–342. 10.1002/9781118029039.
[6] P. Mahat, Z. Chen, B. Bak-Jensen, Review of islanding detection methods for distributed generation, 2008 Third International Conference on Electric Utility Deregulation and Restructuring and Power Technologies, (2008), pp. 2743–2748, https://doi.org/10.1109/drpt.2008.4523877.
[7] M.A. Redfern, O. Usta, G. Fielding, Protection against loss of utility grid supply for a dispersed storage and generation unit, IEEE Trans. Power Del. 8 (3) (1993) 948–954, https://doi.org/10.1109/61.252622.
[8] F.S. Pai, S.J. Huang, A detection algorithm for islanding-prevention of dispersed consumer-owned storage and generating units, IEEE Trans. Energy Convers. 16 (4) (2001) 346–351, https://doi.org/10.1109/60.969474.
[9] J. Vieira, D. Correa, W. Freitas, W. Xu, Performance curves of voltage relays for islanding detection of distributed generators, IEEE Trans. Power Syst. 20 (3) (2005) 1660–1662, https://doi.org/10.1109/tpwrs.2005.852128.
[10] Z. Ye, A. Kolwalkar, Y. Zhang, P. Du, R. Walling, Evaluation of anti-islanding schemes based on nondetection zone concept, IEEE Trans. Power Electron. 19 (5) (2004) 1171–1176, https://doi.org/10.1109/tpel.2004.833436.
[11] A. Timbus, A. Oudalov, C.N.M. Ho, Islanding detection in smart grids, 2010 IEEE Energy Conversion Congress and Exposition, (2010), pp. 3631–3637, https://doi.org/10.1109/ecce.2010.5618306.
[12] J.E. Kim, J.S. Hwang, Islanding detection method of distributed generation units connected to power distribution system, 2000 International Conference on Power System Technology (PowerCon), 2 (2000), pp. 643–647 vol.2.
[13] P. O'Kane, B. Fox, Loss of mains detection for embedded generation by system impedance monitoring, Sixth International Conference on Developments in Power System Protection, (1997), pp. 95–98, https://doi.org/10.1049/cp:19970037.
[14] P. Du, J.K. Nelson, Z. Ye, Active anti-islanding schemes for synchronous-machine-based distributed generators, IEE Proc. Gener. Transm.Distrib. 152 (5) (2005) 597–606, https://doi.org/10.1049/ip-gtd:20045075.
[15] C.G. Bright, COROCOF: comparison of rate of change of frequency protection. a solution to the detection of loss of mains, 2001 Seventh International Conference on Developments in Power System Protection (IEE), (2001), pp. 70–73, https://doi.org/10.1049/cp:20010102.
[16] R.A. Walling, Application of direct transfer trip for prevention of DG islanding, 2011 IEEE Power and Energy Society General Meeting, (2011), pp. 1–3, https://doi.org/10.1109/pes.2011.6039727.
[17] W. Xu, G. Zhang, C. Li, W. Wang, G. Wang, J. Kliber, A power line signaling based technique for anti-islanding protection of distributed generators part i: scheme and analysis, IEEE Trans. Power Del. 22 (3) (2007) 1758–1766, https://doi.org/10.1109/tpwrd.2007.899618.
[18] J. Mulhausen, J. Schaefer, M. Mynam, A. Guzman, M. Donolo, Anti-islanding today, successful islanding in the future, 2010 63rd Annual Conference for Protective Relay Engineers, (2010), pp. 1–8, https://doi.org/10.1109/cpre.2010.5469490.
[19] S. Raza, H. Arof, H. Mokhlis, H. Mohamad, H.A. Illias, Passive islanding detection technique for synchronous generators based on performance ranking of different passive parameters, IET Gener. Transm. Distrib. 11 (17) (2017) 4175–4183, https://doi.org/10.1049/iet-gtd.2016.0806.
[20] R. Leelaruji, L. Vanfretti, M.S. Almas, Voltage stability monitoring using sensitivities computed from synchronized phasor measurement data, 2012 IEEE Power and Energy Society General Meeting, (2012), pp. 1–8, https://doi.org/10.1109/pesgm.2012.6344838.
[21] Y.C. Chen, A.D. Dominguez-Garcia, P.W. Sauer, Measurement-based estimation of linear sensitivity distribution factors and applications, IEEE Trans. Power Syst. 29 (3) (2014) 1372–1382, https://doi.org/10.1109/tpwrs.2013.2292370.
[22] C. Mugnier, K. Christakou, J. Jaton, M.D. Vivo, M. Carpita, M. Paolone, Model-less/measurement-based computation of voltage sensitivities in unbalanced electrical distribution networks, 2016 Power Systems Computation Conference (PSCC), (2016), pp. 1–7, https://doi.org/10.1109/pscc.2016.7540852.
[23] P. Li, H. Su, C. Wang, Z. Liu, J. Wu, PMU-Based estimation of voltage-to-power sensitivity for distribution networks considering the sparsity of Jacobian matrix, IEEE Access 6 (2018) 31307–31316, https://doi.org/10.1109/access.2018.2841010.
[24] R. Schafer, What is a Savitzky-Golay filter? [lecture notes], IEEE Signal Process. Mag. 28 (4) (2011) 111–117, https://doi.org/10.1109/msp.2011.941097.
[25] L. Ljung, System Identification: Theory for the User, Prentice Hall Information and System Sciences Series, Prentice Hall PTR, second edition, pp. 363–364. 10.23919/acc.2004.1384745.
[26] J. Jiang, Y. Zhang, A revisit to block and recursive least squares for parameter estimation, Comput. Electr. Eng. 30 (5) (2004) 403–416, https://doi.org/10.1016/j.compeleceng.2004.05.002.